PHYSICAL REVIEW B VOLUME 48, NUMBER 20 15 NOVEMBER 1993-II

Coulomb attraction in the optical spectra of quantum disks

B. Adolph, S. Glutsch, and F. Bechstedt
Friedrich-Schiller-Universität, Institut für Festkörpertheorie und Theoretische Optik, Max-Wien-Platz 1, D-07743 Jena, Germany
(Received 21 June 1993)

In this paper we present a theory that describes the influence of the Coulomb interaction between electrons and holes on the optical spectra of flat quantum dots within the envelope-function formalism. Starting from a nonlocal Elliott-like formula, absorption and luminescence characteristics are traced back to properties of two-particle wave functions and energies, which are solutions of the corresponding Schrödinger equation for an electron-hole pair under the influence of the Coulomb attraction and confinement potentials, determined by the spatial variation of the band edges of the considered microstructure. We present a complete numerical solution of the two-particle problem for flat quantum dots, i.e., disks for which the size quantization in the growth direction is much stronger than that in the perpendicular plane. The resulting theoretical line shapes are compared with luminescence spectra obtained recently for quantum dots fabricated by laser-induced thermal cation interdiffusion in quantum-well structures.

I. INTRODUCTION

Crystal-growth techniques together with nanometer lithographic techniques have made it possible to fabricate various semiconductor microstructures,[1] among them quasi-zero-dimensional (0D) quantum dot or box systems. The recent technological progress has allowed the study of dots with tailored geometries. The size stochastics[2] appearing in the earlier systems of semiconductor microcrystallites embedded in some host materials, e.g., glass, can now be avoided. A very interesting preparation technique in this respect is the focused-laser-induced thermal cation interdiffusion of narrow quantum-well structures.[3] The interdiffused regions induce lateral barriers for the electron and hole motion. The form of the laser lines determines the resulting microstructure, e.g., a flat quantum wire or quantum disk.

The spectroscopy of optical interband transitions across the band gap, in particular photoluminescence, is a powerful tool to study these systems. Their photoluminescence spectra are governed by efficient intrinsic radiation of free excitons, and exhibit a superior optical performance.[3,4] Studying the development of the corresponding line spectra, one can learn about the mutual interaction of excited electrons (e) and holes (h) and its interplay with vertical and lateral confinement potentials.[5] This holds especially for the increase of the Coulomb interaction due to the confinement, resulting in enhanced oscillator strengths and room-temperature stability of the excitons.

Many theoretical studies have been devoted[6–23] to exciton states in microcrystals. Most of them are related to variational studies of the excitonic ground state in spherical dots or to calculations in some limiting case.[6–14] Typically, infinite barriers are considered. Only a few papers[13,14] consider the incompleteness of the confinement. A full numerical analysis of this problem is done by Hu and co-workers,[15,16] expanding the excitonic wave functions in terms of solutions of the single-particle Schrödinger equations. There are also papers studying nonspherical dots, e.g., boxes,[17] square flat plates,[18] and cylindrical quantum dots.[19,20] Effects such as dielectric confinement and electron-hole exchange interaction on excitonic states in semiconductor quantum dots are also studied.[21] Furthermore, some authors[22,23] have tried to include the complicated structure of the top of the valence band.

In this paper, we follow the line of studying cylindrical quantum dots. However, we solve the excitonic problem of the ground state as well as excited states completely numerically. Solutions for wave functions and energies are used to calculate optical properties, in particular the excitonic luminescence, for flat dots, i.e., disks, which have been observed recently.[3] In Sec. II, the basic equations are given. We define the relevant optical quantities starting from a spatially nonlocal susceptibility. This is related to wave functions and energies of the electron-hole pair equation. In Sec. III, an explicit solution for the electron-hole problem in single quantum disks is described for different dot confinements and strong confinement in the growth direction of the structure. The quantization of the center-of-mass motion and the influence of the disk confinement on the 2D excitons are separately studied. We discuss exciton energies, wave functions, and oscillator strengths versus the disk radius. Optical spectra are explicitly calculated. The results are compared with recent luminescence measurements for disks fabricated by laser-induced cation interdiffusion of narrow quantum wells. Finally, in Sec. IV a short summary is given.

II. BASIC EQUATIONS

A. Optical spectra and exciton states

For systems in which the spatial variation of the photon propagator may be neglected, optical properties can be expressed in terms of a frequency-dependent optical

0163-1829/93/48(20)/15077(9)/$06.00

susceptibility

$$\chi(\omega)=\frac{1}{V}\int_V d\mathbf{x}\int_V d\mathbf{x}'\chi(\mathbf{x},\mathbf{x}';\omega)\ , \tag{1}$$

where the integration runs over the optically active volume V. However, when the lateral structure of a certain dot array as well as the vertical layers in the system should also be taken into account, certain field distribution functions appear in expression (1). Both the absorption coefficient of the transmitted light and the intensity of the luminescence light emitted spontaneously can be related to the imaginary part of the susceptibility (1).[5] In the absorption case, $\mathrm{Im}\chi(\omega)$ can directly be used to describe the spectrum. In the luminescence case, more strictly for an optically pumped semiconductor structure in the quasiequilibrium regime, that is nearly characterized by a sum $\Delta\mu$ of the quasichemical potentials for electrons and holes with respect to the gap center, the frequency dependence of the emitted light is nearly described by $\mathrm{Im}\chi(\omega)$ multiplied with a Bose function $g(\hbar\omega-\Delta\mu)$.[24]

The space-dependent optical function appearing in Eq. (1) can be related directly to the electron-hole pair wave functions $\Phi_\alpha(\mathbf{x}_e,\mathbf{x}_h)$ and energies E_α, with α as the complete set of quantum numbers for the two-particle problem[24,25]

$$\chi(\mathbf{x},\mathbf{x}';\omega)=\frac{2}{\varepsilon_0}|\mu|^2\sum_\alpha\frac{\Phi_\alpha(\mathbf{x},\mathbf{x})\Phi_\alpha^*(\mathbf{x}',\mathbf{x}')}{E_\alpha-\hbar(\omega+i\Gamma_\alpha)}\ . \tag{2}$$

In general, the dipole matrix elements $|\mu|$ contains the complete polarization-vector dependence of the problem. We assume that the optical dipole transition is allowed and nearly state independent. Its polarization dependence is not discussed in detail below. ε_0 denotes the vacuum dielectric constant, and Γ_α indicates a certain damping of the electron-hole pairs.

In the framework of the effective-mass approximation and masses $m_e(m_h)$ of electrons (holes), the electron-hole pairs obey a Schrödinger equation of the form

$$\left\{E_g+\sum_{i=e,h}\hat{H}_i(\mathbf{x}_i)-\frac{e^2}{4\pi\varepsilon_0\varepsilon|\mathbf{x}_e-\mathbf{x}_h|}\right\}\Phi_\alpha(\mathbf{x}_e,\mathbf{x}_h)$$
$$=E_\alpha\Phi_\alpha(\mathbf{x}_e,\mathbf{x}_h)\ , \tag{3}$$

where electrons and holes interact via a Coulomb attraction potential screened by a relative static dielectric constant ε of the underlying semiconductor material forming the disks. Complications in the screening due to the realistic layered and lateral structure of the system[21,26] are avoided, assuming that the dielectric constants of disk and barrier materials are not so very different as in the case of GaAs and $Al_xGa_{1-x}As$. E_g denotes the energy of the allowed optical transition in the underlying bulk material. The single-particle Hamiltonians for electron and hole in Eq. (3) are $(i=e,h)$

$$\hat{H}_i(\mathbf{x}_i)=-\frac{\hbar^2}{2}\nabla_{\mathbf{x}_i}\frac{1}{m_i}\nabla_{\mathbf{x}_i}+W_i(\mathbf{r}_i)+V_i(z_i)\ . \tag{4}$$

For the sake of simplicity the potential that confines carriers in the quasi-0D structures under consideration is written as a sum. The confinement in growth direction z of the quantum-well structure is represented by the potentials $V_i(z_i)$. The lateral confinement in the disks perpendicular to the growth axis is described by the potential $W_i(\mathbf{r}_i)$, with $\mathbf{r}_i=(x_i,y_i,0)$ as a vector in the corresponding horizontal plane.

B. Specification for flat dots (disks)

Following the preparation method described in Ref. 3, one has a situation in which the thickness of the underlying quantum wells, e.g., 30 Å, is much smaller than the lateral extent of the disks. In this strong confinement limit in the z direction, it is convenient to expand the optical susceptibility (2) and, respectively, the pair functions $\Phi_\alpha(\mathbf{x}_e,\mathbf{x}_h)$ in terms of the wave functions $\varphi_{in}(z_i)$ $(i=e,h;\ n=1,2,3,\ldots)$ for the vertical electron and hole motions in the potential $V_i(z_i)$. For spectroscopic reasons these expansions can be restricted to the $n=1$ subbands of electrons and holes in the quantum-well structure. More strictly speaking, we only study the most interesting spectral region of the first heavy-hole–to–conduction-band transition. The corresponding exciton peak is well separated from all others.[3] As a result, pair equation (3) can be rewritten for motions in the xy plane. The important change in the resulting equation concerns the Coulomb potential averaged in the growth direction:

$$v(r)=-\frac{e^2}{4\pi\varepsilon_0\varepsilon}\int_{-\infty}^{+\infty}dz\frac{w(z)}{\sqrt{r^2+z^2}}\ ,$$
$$w(z)=\int_{-\infty}^{+\infty}dZ\,|\varphi_{e1}(Z+\tfrac{1}{2}z)|^2|\varphi_{h1}(Z-\tfrac{1}{2}z)|^2\ . \tag{5}$$

According to Zimmermann[27] the normalized weight can nearly be replaced by a step function $w(z)=1/(2z_0)\Theta(z_0-|z|)$, at least in the strong-localization limit. Then one has $v(r)=-e^2/(4\pi\varepsilon_0\varepsilon z_0)\mathrm{arcsinh}(z_0/r)$, which seems to be reasonable for not too thick quantum wells. For infinite barriers $z_0\approx 0.4L$ (L is the thickness of the well) approximately holds. This means that since the characteristic values for r are of the order of the excitonic Bohr radius or the disk extent, the averaged Coulomb potential can usually be replaced by the 2D one, $v(r)=-e^2/(4\pi\varepsilon_0\varepsilon r)$.

Since the Coulomb attraction of electron and hole, $v(r)$, depends only on a relative coordinate, the introduction of center-of-mass (c.m.) and relative coordinates

$$\mathbf{R}=\frac{m_e}{M_0}\mathbf{r}_e+\frac{m_h}{M_0}\mathbf{r}_h\ ,\quad \mathbf{r}=\mathbf{r}_e-\mathbf{r}_h\ , \tag{6}$$

$$M_0=m_e+m_h\ ,\quad m_0=m_em_h/M_0 \tag{7}$$

should be helpful. With E_g^{2D} as the energetical distance of first heavy-hole and first electron well subband, and a reduced set of quantum numbers β, the Schrödinger equation for the pair motion in the xy plane follows from Eq. (3) to be

$$\left\{E_g^{2D}-\frac{\hbar^2}{2M_0}\nabla_{\mathbf{R}}^2-\frac{\hbar^2}{2m_0}\nabla_{\mathbf{r}}^2+W_e\left[\mathbf{R}+\frac{m_h}{M_0}\mathbf{r}\right]+W_h\left[\mathbf{R}-\frac{m_e}{M_0}\mathbf{r}\right]+v(r)\right\}\Phi_\beta(\mathbf{R},\mathbf{r})=E_\beta\Phi_\beta(\mathbf{R},\mathbf{r})\ . \tag{8}$$

The optical susceptibility (1) can be rewritten as a sum over oscillators:

$$\chi(\omega)=\frac{2}{\varepsilon_0 V}|\mu|^2\sum_\beta\frac{f_\beta}{E_\beta-\hbar(\omega+i\Gamma_\beta)}\ , \tag{9}$$

with oscillator strengths

$$f_\beta=\left|\int d\mathbf{R}\,\Phi_\beta(\mathbf{R},0)\right|^2\ . \tag{10}$$

We mention that in the quasi-0D case expression (9) replaces the Elliott formula well known for the 3D and 2D cases.[28,29]

C. Lateral confinement

The excitons are considered to be optically excited in an isolated cylindrical quantum dot of lateral radius r_0. According to the preparation technique of Ref. 3, the typical dot material is GaAs. Such a disk is embedded in another infinitely large semiconductor layer with a higher energy gap. This barrier material is $Ga_{1-x}Al_xAs$. However, the Al mole fraction x is a function of the distance from the dot center. Because of the preparation by means of cation interdiffusion, there is no sharp transition from the dot to the surroundings. Rather, there is a smooth transition from the band-edge positions in the barrier material to those within the dot. The maximum variation is defined by the band discontinuities between GaAs and the alloy of the well barriers, but somewhat modified by the quantum size effects already present in the underlying well structure. The smooth potentials can be expanded in a power series. For symmetry reasons one obtains (ν even)

$$W_i(\mathbf{r}_i)=\sum_{\nu=2}^{\infty}\alpha_{i\nu}(r_i/r_0)^\nu\ . \tag{11}$$

In explicit calculations we consider only one term $\nu=\nu_0$ of expansion (11). In this way limiting cases of important dot potentials can be derived. The $\nu_0=2$ term gives rise to a parabolic disk. Excitons in spherical dots with parabolic confinement have already been discussed,[30,31] but not excitons in disks. By means of terms with a power $\nu_0\gg1$ the infinite barrier potential can be modeled. Typically we use values $\nu_0=16$, for which convergence in energy eigenvalues is essentially reached. The reason is that the complete numerical analysis of the pair equation (8) is much simpler for smooth potentials $\sim(r_i/r_0)^{\nu_0}$ than for a steplike potential. On the other hand, the preparation by means of laser-induced interdiffusion seems always to produce smooth potentials but not sharp barriers. Another advantage of a potential in power form with a certain ν_0 is the unique splitting of the electron and hole confinement potentials,

$$W_e(\mathbf{r}_e)+W_h(\mathbf{r}_h)=V_{\text{c.m.}}(R)+V_{\text{rel}}(r)+V_{\text{int}}(R,r,\Phi-\varphi)\ , \tag{12}$$

with

$$V_{\text{c.m.}}(R)=W_e(R)+W_h(R)\ ,$$

$$V_{\text{rel}}(r)=W_e\left[\frac{m_h}{M_0}r\right]+W_h\left[-\frac{m_e}{M_0}r\right]\ , \tag{13}$$

$$V_{\text{int}}(R,r,\Phi-\varphi)=W_e(\mathbf{r}_e)+W_h(\mathbf{r}_h)-V_{\text{c.m.}}(R)-V_{\text{rel}}(r)\ ,$$

into confining potentials for the center-of-mass motion, $V_{\text{c.m.}}(R)$, as well as the relative motion, $V_{\text{rel}}(r)$, and a coupling term of the two motions depending on the angles Φ and φ of the two vectors $\mathbf{R}$ and $\mathbf{r}$ with a certain axis in the plane of the disk.

In special cases, such as parabolic disks with equal single-particle quantization energies for electrons and holes, the coupling V_{int} between c.m. and relative motion vanishes.[30,31] In agreement with the "generalized Kohn's theorem,"[32–34] the two motions are separable and the equation for the c.m. motion can be exactly solved. The explicit separability of r and R coordinates in Eq. (8), and the independence of this particular potential of the angles Φ and φ, means that the excitonic wave function can be written as a product. In order to attack the real problem we neglect the coupling of the two motions in a first step. The total two-particle wave function remains separable. The angular wave functions are $(1/\sqrt{2\pi})e^{iM\Phi}$ and $(1/\sqrt{2\pi})e^{im\varphi}$ with $M,m=0,\pm1,\pm2,\ldots$. The radial parts with certain radial quantum numbers N and n as well as eigenvalues E_{NM} and ε_{nm} obey the equations

$$\left\{-\frac{\hbar^2}{2M_0}\left[\frac{d^2}{dR^2}+\frac{1}{R}\frac{d}{dR}-\frac{M^2}{R^2}\right]+V_{\text{c.m.}}(R)-E_{NM}\right\}\Psi_{NM}(R)=0\ , \tag{14}$$

$$\left\{-\frac{\hbar^2}{2m_0}\left[\frac{d^2}{dr^2}+\frac{1}{r}\frac{d}{dr}-\frac{m^2}{r^2}\right]+V_{\text{rel}}(r)+v(r)-\varepsilon_{nm}\right\}\psi_{nm}(r)=0\ .$$

The exact solutions of the pair equation (8) can be expanded in terms of the functions obtained without coupling. One has

$$\Phi_\beta(\mathbf{R},\mathbf{r})=\sum_{N,n}\sum_{M,m}c^\beta_{Mm}(N,n)\Psi_{NM}(R)\psi_{nm}(r)\frac{1}{2\pi}e^{i(M\Phi+m\varphi)}. \tag{15}$$

From the definition (10) of the oscillator strengths

$$f_\beta=\left|\sum_{N,n}c^\beta_{00}(N,n)\psi_{n0}(0)\int_0^\infty dR\,R\Psi_{N0}(R)\right|^2 \tag{16}$$

it follows that only the s-like states of the two radial equations with zero angular momentum are needed. The

unknown coefficients $c_{00}^{\beta}(N,n)$ are derived from a system of algebraic equations which results from Eq. (8), with the ansatz (15).

In the explicit calculations we have solved the eigenvalue problems in Eq. (14) by means of a Rayleigh-Ritz-Galerkin method.[35] Arbitrary disk radii r_0 are discussed, although in the experiment[3] only $r_0 \gtrsim a_B$ (a_B is the Bohr radius of the exciton in bulk GaAs) seem to be realized.

III. DISCUSSION

A. Interplay of center-of-mass and relative motions

Figure 1 shows the imaginary part of the optical susceptibility (9) near the energy gap E_g^{2D} between the first electron and first heavy-hole subband in the underlying quantum-well structure. Strong confinement potentials (11) with $\nu_0=16$ are chosen. Their shape is nearly steplike where the barrier at about $|\mathbf{r}_i|=r_0$ ($i=e,h$) approaches very large values. That means we study more or less a very flat disk with strong confinement. Usually GaAs parameters are used.[30] In principal studies we apply symmetry between electron and hole. All quantities are given in excitonic units, i.e., in terms of the exciton binding energy E_B and the Bohr radius a_B of bulk GaAs. For numerical reasons a small line broadening $\hbar\Gamma=0.05E_B$ is assumed, independent of the certain two-particle state.

The spectra in Fig. 1 are plotted for different disk radii r_0. For the largest dots $r_0=100a_B$ the excitonic spectrum of the underlying GaAs quantum well is observed. However, already for dots with radii $r_0=10$ or $5a_B$, which are large compared to the excitonic Bohr radius, strong quantization effects in the center-of-mass motion are observed. A series of blueshifted satellites with smaller oscillator strengths, belonging to higher quantum numbers N, appear.

When the disk radius r_0 decreases, a fine structure occurs, related to the influence of the dot confinement on the internal motion of the electron-hole pairs, as can be already seen for $r_0=5a_B$. The Coulomb degeneracy is lifted. For dot radii close to the Bohr radius, $r_0 \approx a_B$, the spectra changes qualitatively. The disk confinement leads to well-separated peaks. For $r_0 < a_B$ the physical nature of these peaks can be interpreted in terms of uncorrelated electrons and holes. However, their energetical position and, in particular, their strengths are again remarkably influenced by the Coulomb attraction of electrons and holes.

Figure 1 also indicates the effect of the coupling of the center-of-mass and relative motions. Full calculations are indicated by solid lines, whereas spectra without this coupling are plotted as dashed lines. We see that the coupling of the two motions is less important insofar as the disk radius is larger than the Bohr radius. However, if the space for the exciton in the disk is too small for an unperturbed internal motion, i.e., for $r_0 \lesssim a_B$, the coupling becomes more and more important for the description of the optical spectra. That holds in particular for the energetical positions for the peaks. The spectrum without consideration of the coupling is redshifted in comparison to the correct one, which indicates that the neglect of the coupling of the two motions acts like a decrease of the confinement in the disk.

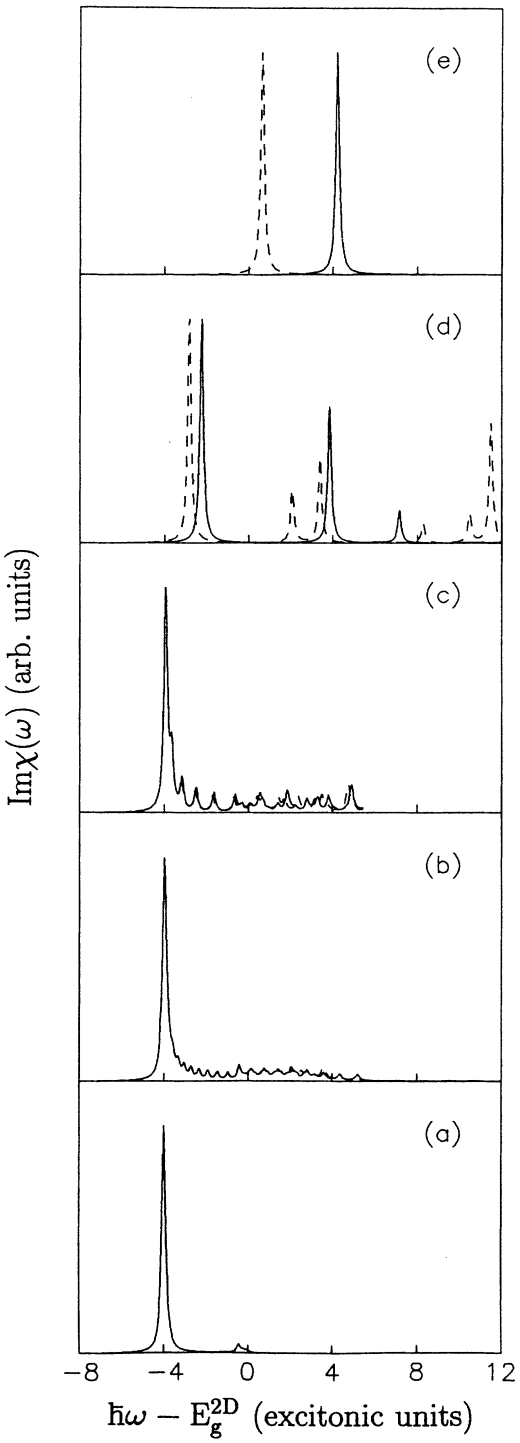

FIG. 1. Imaginary part of the optical susceptibility for different disk radii: $r_0=100$ (a), 10 (b), 5 (c), 1 (d), and $0.5a_B$ (e). Solid lines represent full calculations, dashed lines the same without the coupling of center-of-mass and relative motions. The inverse lifetime of the excitons is fixed at $\hbar\Gamma=0.05E_B$.

B. Correlated versus uncorrelated electron-hole pairs

While the single-particle level spacings due to the disk confinement scale as $1/r_0^2$, the Coulomb term in flat dots scales as $1/r_0$, where r_0 is the characteristic radius of the system. Thus, when the disk size decreases until $r_0 \lesssim a_B$, the Coulomb attraction seems to be treated as a small perturbation. To check this assumption, optical spectra with and without the Coulomb interaction of electrons and holes are plotted in Fig. 2. Indeed, the line spectra in Fig. 2 for $r_0 \leq a_B$ indicate more or less that the peaks arise mainly in the picture of uncorrelated electron-hole pairs, and are only shifted by the Coulomb attraction of electron and hole. The peaks can nearly be characterized by pairs of single-particle quantum numbers of electrons and holes. On the other hand, the most important effect of the Coulomb attraction concerns the oscillator strengths. The Coulomb correlation strongly increases the oscillator strengths, which do not change parallel to the energy. Moreover, the Coulomb shift of the peaks does not follow clear rules.

To study the Coulomb correlation of electron-hole pairs in more detail, we show in Figs. 3 and 4 the pair energies (reduced by the 2D gap) and oscillator strengths for the ground state and the first excited state versus the inverse disk radius $1/r_0$. The principal behavior of the curves in Figs. 3 and 4 versus the size is very similar to that of spherical dots versus the radius.[10,11,13,14,16] We find a strong shift of the pair energies to higher values with the increase in size. The near dependence $\sim 1/r_0^2$ follows that of the single-particle energies in the disk, and is therefore the same as for spherical dots. Most interesting is the Coulomb correlation energy, i.e., the difference of the pair energy and the energy of the uncorrelated electrons and holes. It represents the negative exciton binding energy. For $r_0 \to \infty$ it approaches the value of the underlying 2D exciton, $-4E_B$. In the opposite limit $r_0 \to 0$ it exhibits a nearly linear behavior, $-4E_B - CE_B a_B / r_0$ ($C \approx 3.526$). Hence in the 0D case of small quantum disks the exciton binding energy is divergent, in contrast to the strict 2D case of narrow quantum wells.

The Coulomb enhancement of the oscillator strengths of the first two dipole-allowed optical transitions shown in Fig. 4 behaves like $\sim 1/r_0^2$. This scaling is different from that found for spherical dots, where a size dependence $\sim 1/r_0^3$ is found.[11] This behavior is understandable from the change of the normalization volume of the wave functions.

In light of Fig. 3 there is a question whether the Coulomb correlation of electrons and holes can really be neglected in the small-size limit $r_0 < a_B$, as found for spherical dots,[16] or at least may be treated in perturbation theory.[10] The perturbational treatment of the effect of the Coulomb attraction on the electron-hole-pair ground state is given by the ground-state matrix element v_{1111} of the potential $v(r)$. In the calculation of this Coulomb matrix element the lowest single-particle states of electron and hole appear. In the case of a confinement with infinite barriers, these functions are zero-order Bessel functions $J_0(z_1 r/r_0)$ with $z_1 = 2.404\,82$ as their first zero. One finds

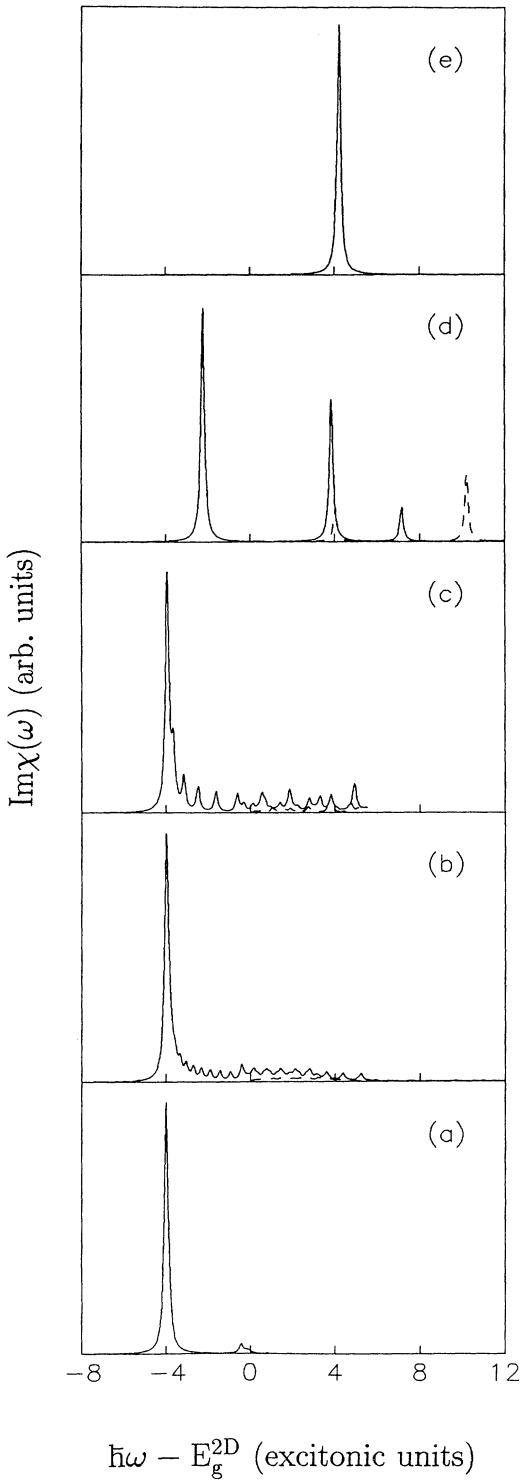

FIG. 2. Imaginary part of the optical susceptibility for different disk radii: $r_0 = 100$ (a), 10 (b), 5 (c), 1 (d), and $0.5a_B$ (e). Solid lines represent calculations under inclusion of the Coulomb attraction, whereas dashed lines give the spectrum for uncorrelated electron-hole pairs. The inverse lifetime of the excitons is fixed at $\hbar\Gamma = 0.05E_B$.

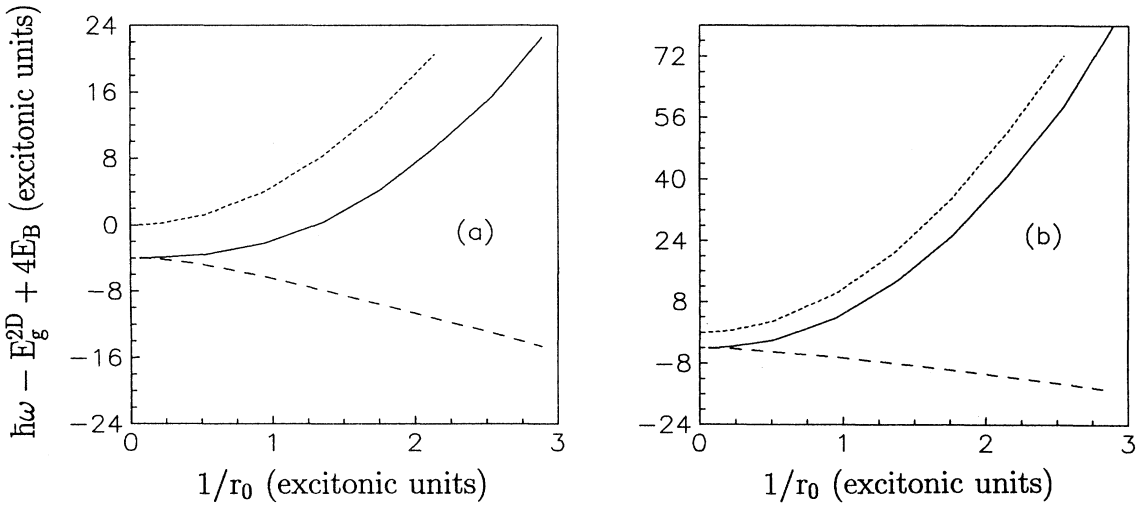

FIG. 3. Energies of excitons in the ground state (a) and the first excited state (b) vs the reciprocal disk radius $1/r_0$ considering (solid line) or neglecting (dotted line) the Coulomb attraction of electron and hole. The difference between the two pair energies, i.e., the Coulomb correlation or negative binding energy of the electron-hole pair, is plotted as a dashed line.

$$v_{1111} = -cE_B a_B / r_0 ,$$
$$c = \frac{1}{2\pi}\left[\frac{\sqrt{2}}{J_0'(z_1)}\right]^4 \int_0^1 dt\, t J_0^2(z_1 t) \times \int_0^1 dt' t' J_0^2(z_1 t') \times \int_0^{2\pi} \frac{d\varphi}{\sqrt{t^2+t'^2-2tt'\cos\varphi}} , \tag{17}$$

with $c \approx 2$. This matrix element underestimates the Coulomb correlation remarkably, even in the limit $a_B > r_0$. The constant $c \approx 2$ is much smaller than that of $C \approx 3.526$ found by the fit of the Coulomb correlation plotted in Fig. 3(a). The perturbation-theory argument cannot be used for the Coulomb effects itself. However, it holds considering the total pair energy, since the confinement energies overcome the Coulomb shifts in the limit $a_B > r_0$.

C. Analytic representation of pair energy

Dependences of the different energy contributions on the disk radii suggest certain approximations. Two different approximations are plotted in Fig. 5, together with exact results (solid line) for the ground-state pair energy and the corresponding oscillator strength versus the reciprocal disk size. In both approximations we assume that the coupling of center-of-mass and internal motions can be neglected. In the first case the equations of motion for both problems are separately solved. The center-of-mass motion is described analytically, whereas the internal motion is treated numerically.

In the second approximation the problem is solved analytically. Because of the neglect of coupling after the coordinate transformation $(r_e, r_h) \rightarrow (R, r)$, the assumption of effective disk radii $r_{0\text{c.m.}}$ and $r_{0\text{rel}}$ of the center-of-mass and relative motions, respectively, different from the geometrical disk radius r_0 of the motions of electron and hole, seems to be reasonable. Practically, the effective disk radii may be considered as variational parameters. The determination of these radii $r_{0\text{c.m.}}, r_{0\text{rel}}$ can result from a physical consideration. Having in mind the total energy of the interaction-free electron-hole pair, we choose $r_{0\text{c.m.}} = r_0/\sqrt{2}$ and $r_{0\text{rel}} = 1.03 r_0$, i.e., effective radii that are reduced with respect to the geometrical one. According to expression (15), we factorize the two-particle wave function

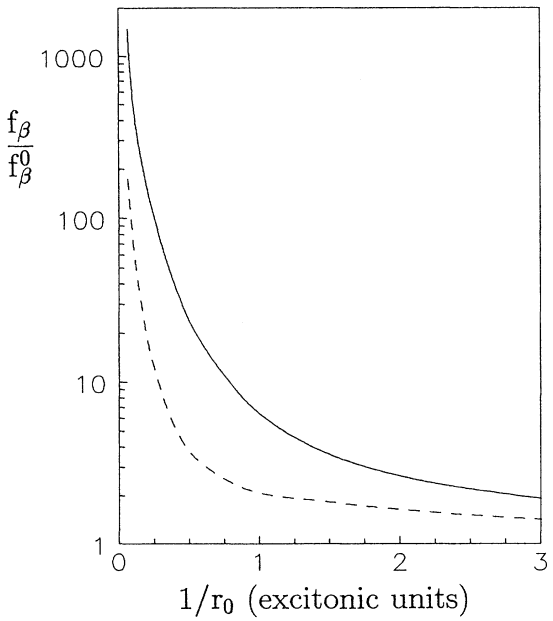

FIG. 4. Coulomb enhancement of the oscillator strength for the ground state (solid line) and the first excited state (dashed line) vs the reciprocal disk radius $1/r_0$. The ratio of the oscillator strength with (f_β) and without (f_β^0) Coulomb correlation is plotted.

$$\Phi_{\text{ground}}(\mathbf{R},\mathbf{r})=\frac{1}{2\pi}\frac{\sqrt{2}}{r_{0\text{c.m.}}J_0'(z_1)}J_0(z_1R/r_{0\text{c.m.}})\frac{1}{a_B}\frac{1}{\sqrt{N(r_{0\text{rel}}/a_B)}}e^{-2r/a_B}(1-r^2/r_{0\text{rel}}^2)\,,$$
$$N(x)=\left[\frac{1}{16}-\frac{3}{64x^2}+\frac{15}{512x^4}-\left[\frac{1}{8x}+\frac{3}{16x^2}+\frac{15}{128x^3}+\frac{15}{512x^4}\right]e^{-4x}\right] \tag{18}$$

into a center-of-mass motion confined in an infinite-barrier disk, and an internal motion of the electron-hole pair, described by a modified 1s wave function of the underlying 2D exciton. Both wave functions vanish at the disk boundary and are normalized to the disk area. The resulting pair energy is

$$E_{\text{ground}}=E_g^{2\text{D}}+E_B\left\{-4+6\left[\frac{a_B}{r_{0\text{rel}}}\right]^2+\frac{m_0}{M_0}\left[\frac{z_1a_B}{r_0}\right]^2\right\}$$
$$-4+\frac{1}{N(x)}\left[\frac{3}{32x^4}-\left[\frac{1}{x}+\frac{3}{4x^2}+\frac{3}{8x^3}+\frac{3}{32x^4}\right]e^{-x}\right]_{x=r_{0\text{rel}}/a_B}+\frac{m_0}{M_0}\left[\frac{z_1a_B}{r_{0\text{c.m.}}}\right]^2, \tag{19}$$

whereas the corresponding oscillator strength can be written as

$$f_{\text{ground}}=\frac{1}{2\pi N(r_{0\text{rel}}/a_B)}\left|\frac{1}{J_0'(z_1)}\int_0^1 dt\,tJ_0(z_1t)\right|^2. \tag{20}$$

Figure 5 makes it evident that the coupling of center-of-mass and internal motions does not play an important role in the exciton ground state. This figure, however, also shows that the ansatz (18) for the ground-state wave function represents a reasonable approximation. The resulting pair energy in Eq. (19) fits well the numerical data in the full size interval, $3r_0 \gtrsim a_B$, under consideration in the upper panel of Fig. 5(a). Most interesting is that the leading size dependence of the pair energy is governed in a wide range only by the size-quantization effects, i.e., by a r_0^{-2} law. There is no r_0^{-1} contribution indicating Coulomb effects. They are mainly represented by the $-4E_B$ term resulting from the bonding of electron and hole already in two dimensions. On the other hand, the wave function in Eq. (18), together with the particular choice of the effective disk radii, overestimates the oscillator strength for the excitation of bounded electron-hole pairs in the ground state [cf. Fig. 5(b)]. The reason seems to be the insufficient description of the wave function for the relative motion for small disk radii $r_0 < a_B$. In this limit we expect a behavior which is better described by an exponential wave function and, therefore, gives rise to a different normalization constant.

D. Luminescence

The imaginary part of the optical susceptibility Eq. (9) multiplied with a certain occupation factor is plotted in Fig. 6 for different effective dot radii r_0, and homogeneous lifetime broadenings Γ of the electron-hole pairs. The damping parameter depends on the disk radius because of the thickness fluctuations in the underlying quantum-well structure.[3] In the case of small disks the

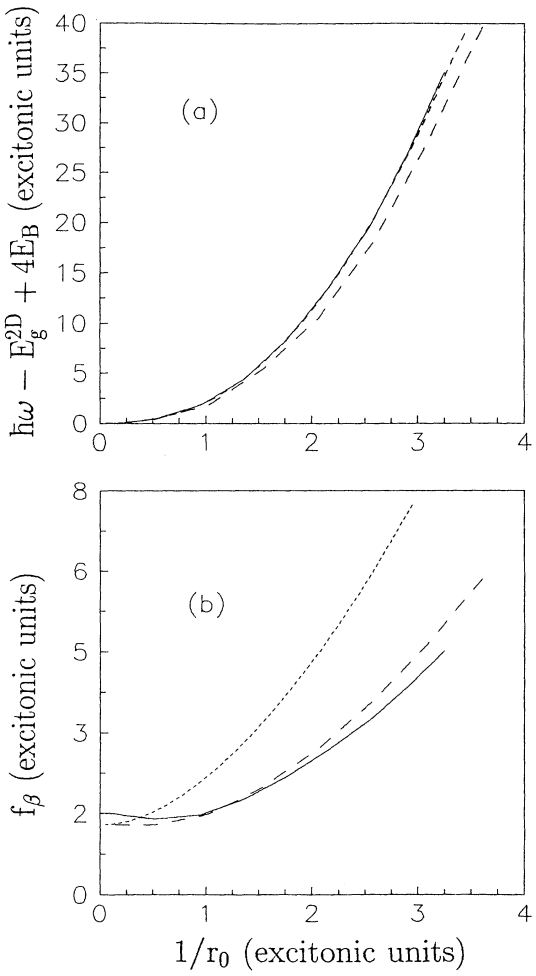

FIG. 5. Ground-state energy (a) and oscillator strength (b) of the exciton vs the reciprocal disk radius $1/r_0$. Solid line: full numerical analysis; dashed line: analytic description of center-of-mass motion and numerical treatment of the internal motion (coupling of both motions are neglected); dotted line: approximate expressions (19) and (20), respectively.

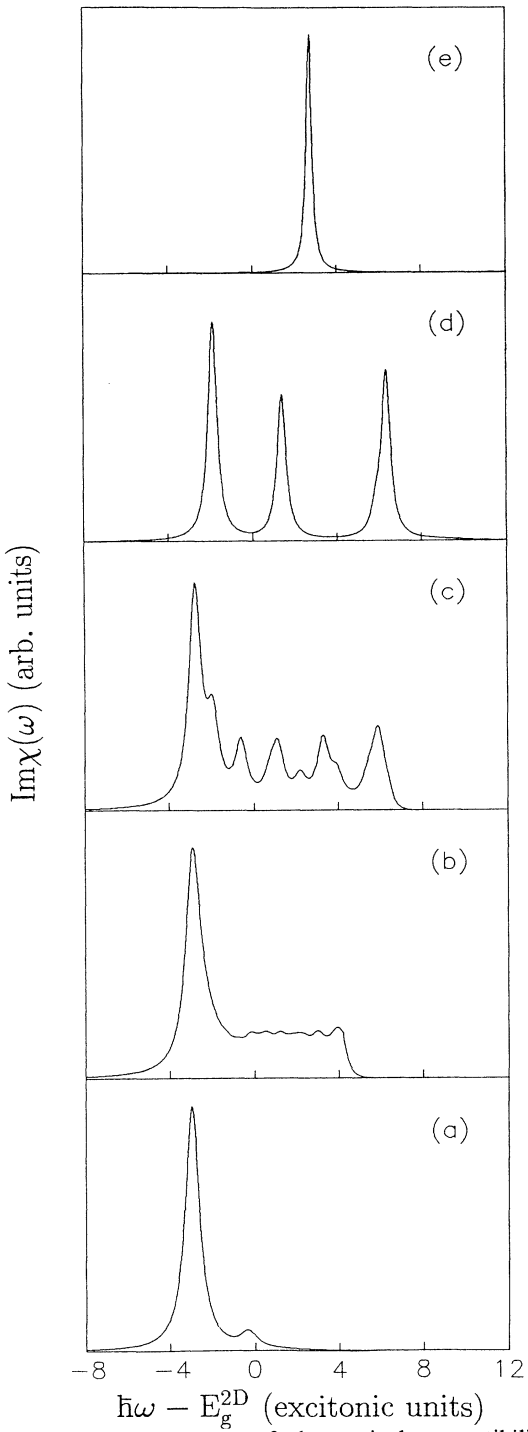

FIG. 6. Imaginary part of the optical susceptibility for different disk radii $r_0=100$ (a), 5 (b), 2 (c), 1 (d), and $0.5a_B$. To compare with experimental luminescence results, a more realistic description of the spectra is attempted. The extent of the underlying quantum well is chosen to be $z_0=0.12a_B$, and the quasi-2D Coulomb potential of Eq. (5) is described by $v(r)=-2E_B/z_0\text{arcsinh}(z_0/r)$. The spectra are cut at the high-energy side by $6.32E_B$ above the lowest exciton peak to model the occupation due to photoexcitation. A size dependence of the damping is taken into account in the form $\Gamma=\frac{1}{5}E_B[1-e^{-r_0/a_B}]$.

exciton feels only a minor number of thickness fluctuations, whereas this effect increases with the disk radius. To plot the spectra we assume a size dependence in the form $\Gamma=\frac{1}{5}E_B[1-e^{-r_0/a_B}]$. The occupation factor is replaced by a step function, since we will compare with low-temperature data. It omits higher frequencies which do not appear in the luminescence due to the occupation.

The series of theoretical spectra in Fig. 6 is in qualitative agreement with the luminescence measurements of Brunner *et al.*[3] This holds in principle with respect to the position and number of peaks. However, to compare theoretical curves with experimental results one has to take into account the following facts: (i) Because of the finite height of the fabricated disks, spectral lines cannot be observed up to arbitrary high energies corresponding to the eigenvalues in the denominator of Eq. (9). On the other hand, the spectra are truncated by the occupation of the electron-hole pair states which is in general governed by the Bose function discussed above. Therefore the choice of the magnitude of the band offsets is of minor influence on the observed spectra. (ii) Due to the thermodiffusion profile, the dot radii entering the confinement potentials do not coincide with the geometrical ones, i.e., the disk boundary fixed by the laser scan lines. The difference is about 200 nm. (iii) For small dot radii we are faced with a superposition of the diffusion tails from the left and right sides and, therefore, the Al content no longer remains at zero inside the dot. Thus the confinement potentials are increased, leading to a blueshift of the spectrum as observed experimentally.

IV. SUMMARY

In conclusion, we have demonstrated the transition from the complete 2D exciton in an extremely narrow quantum well to quasi-0D excitons in well-separated quantum disks prepared on the basis of a narrow quantum well by laser-induced cation interdiffusion. This transition is characterized by the interplay of the center-of-mass motion of the electron-hole pair, its internal motion associated with exciton binding, and the confinement of electron and hole due to the disk potential. Results obtained are applied to describe the optical properties, in particular the photoluminescences of quantum disks.

In the case of flat disks with characteristic radii r_0 and infinite barriers in the disk plane, the strengths of the different effects can be discussed by comparing r_0 with the exciton Bohr radius a_B. In a wide range of disk sizes, $r_0 \gtrsim a_B$, the coupling of center-of-mass and internal motions plays a minor role. Only in the limit of strong confinement, $r_0 < a_B$, the consideration of this coupling is necessary. For $r_0 \gg a_B$ the 2D exciton peak splits due to the quantization of the center-of-mass motion. The oscillator strength is distributed over the different peaks belonging to the symmetric states of the center-of-mass motion. Moreover, a blueshift of the main peak appears. The relative motion of the electron and hole remains 2D-like. In the region $r_0 \gtrsim a_B$ the Coulomb degeneracy in the relative exciton motion is lifted, and a fine structure appears in the spectra. When the disk confinement

effects overcome the Coulomb effects, i.e., when $r_0 < a_B$, the resulting spectra are similar to those obtained without excitonic effects. However, the Coulomb attraction again makes an important enhancement of the oscillator strengths and gives rise to a divergent Coulomb shift $\sim 1/r_0$, even if it is weaker than the size quantization effects $\sim 1/r_0^2$.

Our results are applied to qualitatively explain recent photoluminescence spectra of single disks of varying size. The development of the photoluminescence near the lowest heavy-hole exciton of the underlying quantum well is interpreted in terms of the interplay of excitonic effects and disk confinement. However, a more quantitative analysis of the experimental spectra requires the inclusion of matrix element effects, the fluctuations in the vertical and lateral sizes, and, in particular, more realistic confinement potentials which more strictly reflect the interdiffusion profile.

ACKNOWLEDGMENTS

We would like to thank G. Abstreiter and K. Brunner for helpful discussions and for providing unpublished photoluminescence spectra. Part of this work was supported by the Sonderforschüngsbereich 196 of the Deütsche Forschungsgemeinschaft.

[1]K. Kash, J. Lumin. **46**, 69 (1990).
[2]S. W. Koch, Y. Z. Hu, B. Fluegel, and N. Peyghambarian, in *Proceedings of the International Meeting on Optics of Excitons in Confined Systems,* edited by A. D'Andrea, R. Del Sole, R. Girlanda, and A. Quattropani, IOP Conf. Proc. No. 123 (Institute of Physics and Physical Society, London, 1992), p. 109.
[3]K. Brunner, G. Abstreiter, M. Walther, G. Böhm, and G. Tränkle, Surf. Sci. **267**, 218 (1992); K. Brunner, U. Bockelmann, G. Abstreiter, M. Walther, G. Böhm, G. Tränkle, and G. Weimann, Phys. Rev. Lett. **69**, 3216 (1992).
[4]C. Weisbuch, in *Physics and Application of Quantum Wells and Superlattices,* edited by E. E. Mendez and K. von Klitzing (Plenum, New York, 1987), p. 261.
[5]S. Glutsch and F. Bechstedt, Phys. Rev. B **47**, 4315 (1993); **47**, 6385 (1993).
[6]Al. L. Efros and A. L. Efros, Fiz. Tekh. Poluprovodn. **16**, 1209 (1982) [Sov. Phys. Semicond. **16**, 772 (1982)].
[7]L. E. Brus, J. Chem. Phys. **80**, 4403 (1984).
[8]A. I. E. Kimov, A. L. Efros, and A. A. Onushchenko, Solid State Commun. **56**, 921 (1985).
[9]H. M. Schmidt and H. Weller, Chem. Phys. Lett. **129**, 615 (1986).
[10]S. V. Nair, S. Sinha, and K. C. Rustagi, Phys. Rev. B **35**, 4098 (1987).
[11]Y. Kayanuma, Phys. Rev. B **38**, 9797 (1988).
[12]J. B. Xia, Phys. Rev. B **40**, 8500 (1989).
[13]Y. Kayanuma and H. Momiji, Phys. Rev. B **41**, 10 261 (1990).
[14]D. B. Tran Thoai, Y. Z. Hu, and S. W. Koch, Phys. Rev. B **42**, 11 261 (1990).
[15]Y. Z. Hu, S. W. Koch, M. Lindberg, N. Peyghambarian, E. L. Pollock, and F. F. Abraham, Phys. Rev. Lett. **64**, 1805 (1990).
[16]Y. Z. Hu, M. Lindberg, and S. W. Koch, Phys. Rev. B **42**, 1713 (1990).
[17]R. Del Sole and A. D'Andrea, in *Optical Switching in Low-Dimensional Systems,* edited by H. Haug and L. Banyai (Plenum, New York, 1989), p. 289.
[18]G. W. Bryant, Phys. Rev. Lett. **59**, 1140 (1987); Phys. Rev. B **37**, 8763 (1988); **41**, 1243 (1990).
[19]Y. Kayanuma, Phys. Rev. B **44**, 13 085 (1991).
[20]S. Le Goff and S. Stébé, Phys. Rev. B **47**, 1383 (1993).
[21]T. Takagahara, Phys. Rev. B **47**, 4569 (1993).
[22]Al. L. Efros, in *Proceedings of the International Meeting on Optics of Excitons in Confined Systems* (Ref. 2), p. 147.
[23]S. W. Koch, Y. Z. Hu, B. Fluegel, and N. Peyghambarian, J. Cryst. Growth **117**, 592 (1992).
[24]R. Zimmermann, *Many-Particle Theory of Highly Excited Semiconductors* (Teubner-Verlag, Leipzig, 1987).
[25]H. Haug and S. W. Koch, *Quantum Theory of the Optical and Electronic Properties of Semiconductors* (World Scientific, Singapore, 1990).
[26]L. Wendler, F. Bechstedt, and M. Fiedler, Phys. Status Solidi B **159**, 143 (1990); Superlatt. Microstruct. **10**, 183 (1991).
[27]R. Zimmermann, Phys. Status Solidi B **135**, 681 (1986).
[28]R. J. Elliott, Phys. Rev. **108**, 1384 (1957).
[29]M. Shinada and S. Sugano, J. Phys. Soc. Jpn. **21**, 1936 (1966).
[30]V. Halonen, in *Proceedings of the International Meeting on Optics of Excitons in Confined Systems* (Ref. 2), p. 313.
[31]Weiming Que, Solid State Commun. **81**, 721 (1992).
[32]L. Brey, N. F. Johnson, and B. I. Halperin, Phys. Rev. B **40**, 10 647 (1989).
[33]P. A. Maksym and T. Chakraborty, Phys. Rev. Lett. **65**, 108 (1990).
[34]F. M. Peeters, Phys. Rev. B **42**, 1486 (1990).
[35]J. Stoer and R. Bulirsch, *Introduction to Numerical Analysis* (Springer, New York, 1983).